

Magnetization and exchange-stiffness constants of Fe-Al-Si alloys at finite-temperatures: A first-principles study

Shogo Yamashita* and Akimasa Sakuma

Department of Applied Physics, Tohoku University, Sendai 980-8579, Japan

(Dated: March 22, 2024)

We investigated the magnetic properties of Sendust (Fe-Al-Si) alloys not only at 0 K but also at finite-temperatures by means of the first-principles calculations assuming A2, B2, and DO3 structures. We confirmed that the itinerant characteristics of 3d electrons of Fe are not negligible for A2 and B2 structures and a significantly small exchange stiffness constant exists at zero-temperature in a B2 structure. However, the calculated Curie temperatures are in the same order for all structures; this indicates that the Curie temperature cannot be determined only by the exchange interactions at zero-temperature in itinerant electron systems. Temperature dependence of the exchange interaction, namely spin configuration dependence, also might be important for determining it. In addition, this property might also be related to the unique behavior of the temperature dependence of the exchange stiffness constant for the B2 structure, which does not decrease monotonically as temperatures increase, contrary to the behavior expected from the Heisenberg model. In addition, we investigated composition dependence on the exchange stiffness constant at zero-temperature and confirmed that the substitution of Si with Al could improve the amplitude of the exchange stiffness constant at zero-temperature for all structures.

I. INTRODUCTION

Magnetic materials are essential materials for sustaining the wide range of modern technology. For instance, hard magnets with strong magnetic anisotropy, such as Nd₂Fe₁₄B, are typical examples of magnetic materials that sustain modern society. Conversely, soft magnetic materials that have weak magnetic anisotropy are also important materials for modern spintronics applications. For instance, Sendust (Fe-Al-Si) alloy is a soft magnetic material comparable with permalloys. Sendust alloy was invented by Masumoto and Yamamoto in 1937[1], and is now used in various applications such as magnetic recording heads. In addition, recently, Akamatsu et al[2–4], showed that Sendust alloy is a promising candidate for the free layers of a magnetic tunnel junction (MTJ)-based magnetic sensor, which can detect external magnetic fields using the tunnel magnetoresistance (TMR) effect. Generally, a high TMR ratio is desired to develop highly sensitive magnetic TMR sensors at room-temperature. However, the TMR ratio is usually temperature dependent and decreases as temperatures increase due to, for instance, the thermal spin fluctuations. Therefore, to sustain a high TMR ratio even at room temperature or above, it is essential to enhance the exchange stiffness constant, which represents the robustness of the exchange couplings of a system, even at finite temperatures.

However, the theoretical description of the temperature dependence of the exchange stiffness constant is still controversial. Phenomenologically, the exchange stiffness constant A can be defined as $f(\vec{r}) = A \sum_{\alpha} (\vec{\nabla} m_{\alpha}(\vec{r}))^2$, where f and m are free energy density and magnetization density, respectively. The theoretical description of the temperature dependence of A has been established, for instance, by Dyson[5] with the Heisenberg Hamiltonian. The recent attempts based on the localized spin model have also been made[6, 7]. However, 3d electrons of transition metals are currently regarded as itinerant

electrons. 3d electrons have dual properties, that of localized magnetic moments and hybridization effects, due to their itinerant nature; moreover, the magnetic moments and effective exchange interactions have environment dependence, for instance, spin-configurations dependence[8–11]. Therefore, the localized spin model is not always suitable to describe itinerant magnets. Thus, we need to establish a theory that can capture both the localized and itinerant properties of 3d electrons to describe the temperature dependence of the exchange stiffness constant of itinerant magnets.

From this perspective, many attempts to establish the spin-fluctuation theory of itinerant electron systems at finite temperatures have already been made[12]. Among them, a convenient theoretical way to describe finite temperature magnetic properties by describing spin-fluctuations of itinerant magnets is the functional integral method combined with the concept of the local moment disorder (DLM) and coherent potential approximations (CPA)[13–18]. This method was originally proposed in the single band Hubbard model and was translated to a first-principles calculation scheme to investigate finite-temperature magnetic properties based on realistic electronic structures[19–23]. Although this scheme is based on static and single-site approximations, recently, it has been applied to calculate the temperature dependence of magnetic anisotropy[24–31], Gilbert damping constant[32, 33], and transport properties[34], and the non-localized spin model like behavior of finite-temperature magnetic properties have been revealed[30]. In addition to these properties, very recently, Sakuma[35] proposed the scheme to calculate the temperature dependence of the exchange stiffness constants of itinerant magnets based on the DLM-CPA scheme. This has enabled the investigation of the temperature dependence of the exchange stiffness constant of itinerant magnets without assuming localized spin model for 3d electrons in metallic systems.

In this study, we aim to investigate the magnetic properties of Fe-Al-Si alloys not only at 0K but also at finite temperatures; in particular, we aim to investigate the temperature dependence of the exchange stiffness constant by using the finite-temperature

* shogo.yamashita.q1@dc.tohoku.ac.jp

itinerant electrons theory based on first-principles calculations with the DLM-CPA scheme.

II. METHOD

We use the functional integral approach together with the local moment disorder picture to investigate the finite-temperature magnetic properties of Fe-Al-Si based on first-principles calculations. We treat the fluctuation of the local moments with the adiabatic approximation due to the slow time scale of the spin fluctuation compared with the motion of electron hopping. The partition function Z and the free energy F of the system are given as follows:

$$Z = \int \left(\prod_i d\mathbf{e}_i \right) e^{-\Omega(T, \{\mathbf{e}\})/k_B T}, \quad (1)$$

$$F = \langle \Omega(T, \{\mathbf{e}\}) \rangle_{\omega(T, \{\mathbf{e}\})} + k_B T \langle \ln \omega(T, \{\mathbf{e}\}) \rangle_{\omega(T, \{\mathbf{e}\})}, \quad (2)$$

where $\Omega(T, \{\mathbf{e}\})$, $\omega(T, \{\mathbf{e}\})$, and \mathbf{e}_i are a thermodynamic potential, a distribution of spin orientation, and an orientation vector of the local spin moment at site i . k_B is a Boltzmann constant. Once we obtain $\Omega(T, \{\mathbf{e}\})$, $\omega(T, \{\mathbf{e}\})$ is given as follows:

$$\omega(T, \{\mathbf{e}\}) = \exp(-\Omega(T, \{\mathbf{e}\})/k_B T) / Z. \quad (3)$$

Here, we neglect the longitudinal fluctuations of local moments. Thus, the integration with respect to \mathbf{e} is only for the freedom of directions. $\langle A \rangle_{\omega(T, \{\mathbf{e}\})}$ is given as follows:

$$\langle A(\{\mathbf{e}\}) \rangle_{\omega(T, \{\mathbf{e}\})} = \int \prod_i d\mathbf{e}_i \omega(T, \{\mathbf{e}\}) A(\{\mathbf{e}\}). \quad (4)$$

In this study, we use the tight-binding linearized muffin-tin orbital (TB-LMTO) method[36–40] to evaluate $\Omega(T, \{\mathbf{e}\})$, which determines spin orientation distribution corresponding to the spin-transverse fluctuations at T . The Green function, including the spin-transverse fluctuation of the system in the TB-LMTO method, is given as follows:

$$\begin{aligned} G_{ij}(z; \{\mathbf{e}\}) &= (z - H_{\text{TB-LMTO}}(\{\mathbf{e}\}))_{ij}^{-1} \\ &= \lambda_i^\alpha(z; \{\mathbf{e}\}) \delta_{ij} + \mu_i^\alpha(z; \{\mathbf{e}\}) g_{ij}^\alpha(z; \{\mathbf{e}\}) \bar{\mu}_j^\alpha(z; \{\mathbf{e}\}), \end{aligned} \quad (5)$$

$$g_{ij}^\alpha(z; \{\mathbf{e}\}) = [(\tilde{P}^\alpha(z; \{\mathbf{e}\}) - S^\alpha)^{-1}]_{ij}, \quad (6)$$

where λ and μ are

$$\lambda_i^\alpha(z; \mathbf{e}_i) = (\tilde{\Delta}_i(\mathbf{e}_i))^{-1/2} (1 + (\tilde{\gamma}_i(\mathbf{e}_i) - \alpha) \tilde{P}_i^\gamma(z; \mathbf{e}_i)) (\tilde{\Delta}_i(\mathbf{e}_i))^{-1/2}, \quad (7)$$

$$\mu_i^\alpha(z; \mathbf{e}_i) = (\tilde{\Delta}_i(\mathbf{e}_i))^{-1/2} (\tilde{P}_i^\gamma(z; \mathbf{e}_i))^{-1} \tilde{P}_i^\alpha(z; \mathbf{e}_i), \quad (8)$$

$$\bar{\mu}_i^\alpha(z; \mathbf{e}_i) = \tilde{P}_i^\alpha(z; \mathbf{e}_i) (\tilde{P}_i^\gamma(z; \mathbf{e}_i))^{-1} (\tilde{\Delta}_i(\mathbf{e}_i))^{-1/2}, \quad (9)$$

$$P_i^\alpha(z) = P_i^\gamma(z) \{1 - [\alpha - \gamma_i] P_i^\gamma(z)\}^{-1}, \quad (10)$$

$$P_i^\gamma(z) = (\Delta_i)^{-1/2} [z - C_i] (\Delta_i)^{-1/2}. \quad (11)$$

Here, γ_i , Δ_i , and C_i are called potential parameters. S^α is given as $S(1 - \alpha S)^{-1}$. S is a bare structure constant. From here, to utilize the CPA, we use the β -representation, regarded as a maximum localized representation, instead of general α representations to express the Green function. β values have been summarized in earlier studies [34, 38, 39]. The Hamiltonian $H_{\text{TB-LMTO}}$ is given as follows:

$$\begin{aligned} H_{\text{TB-LMTO}}(\{\mathbf{e}\}) \\ = \tilde{C}(\{\mathbf{e}\}) + \tilde{\Delta}^{1/2}(\{\mathbf{e}\}) S (1 - \tilde{\gamma}(\{\mathbf{e}\}) S)^{-1} \tilde{\Delta}^{1/2}(\{\mathbf{e}\}). \end{aligned} \quad (12)$$

In this study, we defined $\tilde{A}(\{\mathbf{e}\})$ as follows:

$$\tilde{A}(\{\mathbf{e}\}) = U^\dagger(\{\mathbf{e}\}) A U(\{\mathbf{e}\}), \quad (13)$$

where U is a SU(2) rotation matrix.

The thermodynamic potential of the electronic part $\bar{\Omega}$ is also expressed as follows:

$$\begin{aligned} \bar{\Omega}(T, \{\mathbf{e}\}) \\ = \frac{1}{\pi} \int d\epsilon f(\epsilon, T, \mu) \int_{-\infty}^{\epsilon} dE \text{ImTr} G(z; \{\mathbf{e}\}) \\ = -\frac{1}{\pi} \int d\epsilon f(\epsilon, T, \mu) \text{Im} [\text{Tr} \log \lambda^\beta(\epsilon^+; \{\mathbf{e}\}) + \text{Tr} \log g^\beta(\epsilon^+; \{\mathbf{e}\})], \end{aligned} \quad (14)$$

where f and μ are the Fermi–Dirac function and chemical potential, respectively; here we dropped the double counting part of the exchange–correlation energy part relying on the concept of the magnetic force theorem[41] and evaluated $\omega(T, \{\mathbf{e}\})$ with only the electronic part of $\Omega(T, \{\mathbf{e}\})$. In the actual evaluation of $\bar{\Omega}(T, \{\mathbf{e}\})$, we need to perform the functional integral with respect to various spin configurations composed of multi spins. This is generally impractical and an approximation needs to be made. To obtain $\bar{\Omega}(T, \{\mathbf{e}\})$, we use the coherent potential approximation together with the single-site approximation. In this approximation, it will also be decomposed as follows:

$$\bar{\Omega}(T, \{\mathbf{e}\}) = \bar{\Omega}_0 + \Delta \bar{\Omega}(T, \mathbf{e}_i), \quad (15)$$

and each part is also given as follows:

$$\bar{\Omega}_0 = -\frac{1}{\pi} \int d\epsilon f(\epsilon, T, \mu) \text{Im} [\text{Tr} \log \tilde{g}^\beta(\epsilon^+)], \quad (16)$$

$$\begin{aligned} \Delta \bar{\Omega}(T, \mathbf{e}_i) &= -\frac{1}{\pi} \int d\epsilon f(\epsilon, T, \mu) \text{Im} \left[\text{Tr} \log \lambda^\beta(\epsilon^+) \right. \\ &\quad \left. - \text{Tr} \log (1 + \Delta P(z; \{\mathbf{e}\}) \tilde{g}^\beta(\epsilon^+)) \right], \end{aligned} \quad (17)$$

$$\Delta P(z; \{\mathbf{e}\}) = \tilde{P}^\beta(z; \{\mathbf{e}\}) - \tilde{P}(z). \quad (18)$$

Here, we define \bar{g}^β as follows:

$$\bar{g}^\beta(z) = (\bar{P}(z) - S^\beta)^{-1}, \quad (19)$$

where S^β is also given as $S(1 - \beta S)^{-1}$. To obtain $\bar{P}(z)$, we use the so-called CPA condition. The CPA condition is given as follows:

$$\int d\mathbf{e}_i \omega_i(T, \mathbf{e}_i) \left[1 + \Delta P_i(z; \mathbf{e}_i) \bar{g}_{ii}^\beta(z) \right]^{-1} \Delta P_i(z; \mathbf{e}_i) = 0. \quad (20)$$

Once we have converged $\omega_i(T, \mathbf{e}_i)$, we can obtain \bar{P} in a self-consistent manner using Eqs. (18), (19), and (20). Therefore, we can obtain $\omega_i(T, \mathbf{e}_i)$ as follows:

$$\begin{aligned} \omega_i(T, \mathbf{e}_i) &= \exp(-\Delta\bar{\Omega}_i(T, \mathbf{e}_i)/k_B T) / \int d\mathbf{e}_i \exp(-\Delta\bar{\Omega}_i(T, \mathbf{e}'_i)/k_B T). \end{aligned} \quad (21)$$

In this approximation, $\omega(T, \{\mathbf{e}\})$ is decomposed to the simple product of probability at each site i as $\omega(T, \{\mathbf{e}\}) = \prod_i \omega_i(T, \mathbf{e}_i)$.

To calculate the exchange stiffness constant, we express a spin-spiral magnetic structure[42–46]. In the TB-LMTO scheme, the structure constant \tilde{S} to express spin-spiral states is given as follows[47, 48]:

$$\tilde{S}_{ij}(\vec{k}, \vec{q}) = U_i \begin{pmatrix} S_{ij}(\vec{k} - \frac{\vec{q}}{2}) & 0 \\ 0 & S_{ij}(\vec{k} + \frac{\vec{q}}{2}) \end{pmatrix} U_j^\dagger, \quad (22)$$

where i and j stand for sites of atoms in a primitive unit cell, and we redefine U at site i as follows:

$$U_i = \frac{1}{\sqrt{2}} \begin{pmatrix} e^{i(\frac{\vec{q}}{2} \cdot \vec{r}_i)} & e^{-i(\frac{\vec{q}}{2} \cdot \vec{r}_i)} \\ -e^{i(\frac{\vec{q}}{2} \cdot \vec{r}_i)} & e^{-i(\frac{\vec{q}}{2} \cdot \vec{r}_i)} \end{pmatrix}, \quad (23)$$

where \vec{r}_i denotes atomic positions in a primitive unit cell. We also rely on the concept of the force theorem to obtain the free energy difference. Neglecting the contribution of the second term in Eq. (2) (entropy of the spin configuration) as well as the double counting term, the free energy difference is given as follows:

$$\Delta F(\vec{q}, T) \sim \langle \bar{\Omega}(\vec{q}, T) \rangle - \langle \bar{\Omega}(\vec{q} = 0, T) \rangle, \quad (24)$$

$$\langle \bar{\Omega}(\vec{q}, T) \rangle = \sum_i \int d\mathbf{e}_i \omega_i(\mathbf{e}_i, T) \bar{\Omega}_i(T, \vec{q}, \mathbf{e}_i), \quad (25)$$

$$\begin{aligned} \bar{\Omega}_i(T, \vec{q}, \mathbf{e}_i) &= -\frac{1}{\pi} \text{ImTr}_{L\sigma} \int_{-\infty}^{\infty} d\epsilon \epsilon f(\epsilon, T, \mu) G_{ii}(\epsilon + i\delta, \vec{q}, \mathbf{e}_i) \\ &- \frac{k_B T}{\pi} \text{ImTr}_{L\sigma} \int_{-\infty}^{\infty} d\epsilon G_{ii}(\epsilon + i\delta, \vec{q}, \mathbf{e}_i) \\ &\times (f(\epsilon, T, \mu) \log f(\epsilon, T, \mu) + (1 - f(\epsilon, T, \mu)) \log(1 - f(\epsilon, T, \mu))) \end{aligned} \quad (26)$$

$$\begin{aligned} G_{ii}(z, \vec{q}, \mathbf{e}_i) &= \lambda_i^\beta(z, \mathbf{e}_i) + \mu_i^\beta(z, \mathbf{e}_i) \bar{g}_{ii}^\beta(z, \vec{q}) (1 + \Delta P_i(z, \mathbf{e}_i) \bar{g}_{ii}^\beta(z, \vec{q}))^{-1} \bar{\mu}_i^\beta(z, \mathbf{e}_i), \end{aligned} \quad (27)$$

$$\bar{g}_{ii}^\beta(z, \vec{q}) = \left(\frac{1}{N} \sum_{\vec{k}} (\bar{P}(z) - \tilde{S}^\beta(\vec{k}, \vec{q}))^{-1} \right)_{ii}, \quad (28)$$

where N is a number of \vec{k} -points. Using this free energy difference, the exchange stiffness constant $A_\eta(T)$ is given as follows:

$$A_\eta(T) = \frac{1}{2V} \frac{d^2 \Delta F(\vec{q}, T)}{dq_\eta^2}, \quad (29)$$

where V is the volume of the system, and η is the direction of the spin-spiral. In this study, we fix η to be in the [001] direction ($q_\eta = q_z$). We show the assumed crystal structures of Fe-Al-Si in Fig. 1. In this study, we set the composition of these elements to Fe 75%, Al 12.5%, and Si 12.5% to calculate the finite-temperature magnetic properties. The lattice constant a is set to 2.884 for the A2 and B2 structure and 5.688 for the DO3 structure. We used the local spin density approximation for the exchange correlation potential.

III. RESULTS AND DISCUSSIONS

Initially, we summarize the calculated zero-temperature magnetic properties of Fe-Al-Si alloys. The calculated exchange stiffness constants and magnetic moments of each structure are summarized in Table I. From this table, we can see that the exchange stiffness constant of the B2 structure is significantly small (about one-tenth) compared with that of other structures. We will conduct further investigation regarding this in a latter section. In the B2 structure, the magnetic moment of the Fe1 site is significantly small compared with that of the other site. A similar tendency is confirmed in the Fe1 site in the DO3 structure. This reduction of magnetic moments may be attributed to the hybridization effects of the $3d$ orbitals of Fe1 sites with the $2p$ orbitals of Al or Si. The interatomic distance between Fe1 and Al or Si is $\frac{\sqrt{3}a}{2}$, which is smaller than a , corresponding to the distance between Fe2 and Al or Si. To investigate it, we also performed the self-consistent conventional DLM calculations, which include only spin up and down states for A2 and B2 structures, and calculate the converged magnetic moments of each site. The calculated results are also summarized in Table I. From these results, the significant reduction of the magnetic moments of the Fe1 site of the B2 structure is confirmed; this reflects the itinerant picture of d electrons in Fe1 sites, which have a strong dependence on the environment surrounding the atoms. This situation can be attributed to the electronic state of Fe in the Fe1 site being close to that of fcc Co and

TABLE I. Calculated exchange stiffness constants and magnetic moments at each site of Fe-Al-Si alloys with each structure at ferromagnetic and the DLM states.

System	A [meV/Å]	M_{Fe1} [μ_B]	M_{Fe2} [μ_B]	M_{Fe3} [μ_B]
A2	10.93	2.029	-	-
B2	0.938	1.220	2.325	-
DO3	8.480	1.491	2.372	2.417
DLM A2	-	1.766	-	-
DLM B2	-	0.015	2.438	-

fcc Ni observed in several studies [49–52] and it is owing to the hybridization with the $2p$ orbitals of light elements such as N, B, C and Al or Si in this case. Conversely, the magnetic moments of Fe2 sites are larger than that of bcc-Fe; this can be considered a compensation effect due to the hybridization with the Fe1 $3d$ orbitals, whose exchange splitting is reduced. In the A2 structure, the Fe moments go to an intermediate value because the two effects on Fe1 and Fe2 are weakened.

Next, we investigate the finite temperature magnetic properties of Fe-Al-Si alloys. At first, we show the temperature dependences of the magnetization of Fe-Al-Si alloys for each structure in Fig. 2. The result for the A2 structure, the shape of the total magnetization curve is similar to the Langevin function, which can be expected from the single-site approximation. However, other results do not follow this trend. To examine the reason for this situation, we focus on the temperature dependence of site-resolved magnetization for B2 and DO3 structures. For the B2 and DO3 structures, the behavior of the temperature dependence of magnetization at Fe1 sites in the B2 structure and Fe1 sites in the DO3 structure in Fig. 1 (c) deviates from the Langevin function-like behavior. In addition, the magnetic moments of these sites at 0 K are smaller than that of other sites; the exchange coupling energy J_0 [41] is also smaller than that of other site. As discussed earlier, this may be due to the fact that the magnetic moments on these Fe atoms are easily influenced by environment wherein, they are surrounded by other atoms and the localized characteristics is weakened. Owing to above reasons, the magnetic moments of these sites are sustained by the exchange field from other Fe atoms, not by the intra-atomic Coulomb interaction (Hund coupling) at high temperatures. The calculated Curie temperatures are 1640 K, 1160 K, and 1480 K for the A2, B2, and DO3 structures, respectively. Experimentally, it is reported to be 733 K[53] for $\text{Fe}_{85}\text{Al}_{5.4}\text{Si}_{9.6}$ (wt. %) ($\text{Fe}_{73.7}\text{Al}_{9.7}\text{Si}_{16.6}$ (at. %)). Although the composition is different from our calculation models, our results overestimate the Curie temperature compared with the experimental result. It is noted that as shown by Hiramatsu et al.[32], the Curie temperature of bcc-Fe is approximately 2000 K which is approximately two times larger than the experimental value. Judging from the present data combined with that of the of bcc-Fe, we see that the family of alloys related to bcc-Fe have a trend to exhibit high Curie temperature. Considering this, the lower T_c 's of the Fe-Al-Si alloys compared to the T_c of bcc-Fe may be reasonable since

a part of Fe atoms are substituted by non-magnetic elements such as Al and Si in these alloys. It is worth mentioning that the reduction of the Curie temperature for bcc-Fe due to the phonon excitation has been reported theoretically[54]. In addition, the reduction of the local moment induced by phonon excitation has also been reported by Heine et al.[55] for bcc-Fe. Our case is close to the situation of bcc-Fe, thus it might affect our results. However, these couplings between spin disorders and phonon excitations are not taken into account in our study. Moreover, we used the force theorem approach and the potential parameters are fixed to that of the ferromagnetic ground states. These treatments also might affect our result, in particular for the results of B2 structure.

Moreover, apart from the values of T_c themselves, the fact that the relative values of T_c of these alloys are not proportional to the values of A at $T = 0$ as shown in Table I; that is, the A of B2 structure is extremely smaller compared to those of A2 and DO3 structures, while the T_c of these structures are in the same order is puzzling. These results may indicate that the Curie temperatures of itinerant electron systems are not always determined by the exchange interaction at $T = 0$ but are governed by the temperature variation of the exchange constants. To examine this feature, we calculated the temperature dependence of A of these structures.

Figure 3 shows the calculated results of $A(T)$. The $A(T)$ of A2 and DO3 structures was found to exhibit monotonic decreasing behavior with increasing T , as seen in the measured spin stiffness constant $D(T)$ of bcc-Fe[56]. If one adopts a simple spin model such as the Heisenberg model, where the constant exchange interaction is given, $A(T)$ may decrease with increasing T . Actually, according to Dyson[5], $A(T)$ behaves proportional to $1 - (T/T_c)^{\frac{5}{2}}$ in the low-temperature region owing to the magnon–magnon scattering. However, as seen in Table I, the localized spin picture may not be appropriate for these alloys. Conversely, $A(T)$ of the B2 structure reveals a peak at around 600 K. If one focuses on the behavior of $A(T)$ for $T > 700$ K, the resultant T_c of the B2 structure seems reasonable. It should be emphasized here that, in metallic systems, the exchange interaction itself can vary depending on the spin configuration at each temperature, as reported for basic magnetic materials[9]. This has been confirmed in Heusler alloys[58] and even for a metallic $4f$ electron system.[59] Although our calculations are based on the force theorem, not self-consistent calculations performed in previous works to investigate configuration dependence of the exchange interactions, this effect might seem to be key to explain our result. At this stage, however, why this particular behavior occur only in the B2 structure is not revealed exactly.

To investigate how the Al and Si atoms affect the A of the B2 structure, we examine the Si concentration dependence of A at $T = 0$. The results are shown in Fig. 4 by varying the Fe concentration from 70 to 80 atomic percent. The results clearly indicate that A is significantly sensitive to the Si concentration; that is, A decreases monotonically with decreasing Si concentration or increasing Al concentration. Notably, if the Si concentration is below 10% for $\text{Fe}_{75}\text{Al}_{25-x}\text{Si}_x$ and 15% for $\text{Fe}_{70}\text{Al}_{30-x}\text{Si}_x$, the ferromagnetic state becomes unstable,

and the exchange stiffness constant cannot be defined. We consider that this is attributed to the itineracy of $3d$ electrons due to the strong hybridization between the Fe $3d$ orbitals and Al $2p$ orbitals, whose radius is larger than those of Si atoms. This result may indicate that the concentration of the Al atom is a key of the small exchange stiffness constant of the Fe-Al-Si alloy with the B2 structure.

To investigate how the Al atoms affect the exchange stiffness constant depending on the structure, we also examined the Si concentration dependence of the exchange stiffness constant for Fe-Al-Si with a DO3 structure. The results are shown in Fig. 5. We can see that if we increase the Si concentration, the exchange stiffness constants also increase. A similar trend is also confirmed in the A2 structure; however, the change in amplitude of the exchange stiffness constant is small. From these results, we can conclude that doping of the Al atom leads to a reduction of the exchange stiffness constant for all structures but this trend is most prominent in the B2 structure. Although we took specific alloys in this case, a similar tendency is also experimentally confirmed in Co based Heusler alloys[57]. In Co_2MnSi and Co_2MnAl , $A = 14.7$ meV/ and $A = 2.99$ meV/, respectively. However, the observed Curie temperatures are 985 K and 693 K. The difference between alloys is small compared with that of the exchange stiffness constant, and this tendency is qualitatively consistent with our results.

IV. SUMMARY

In summary, we investigated the magnetic properties of Fe-Al-Si alloy not only at zero-temperature but also at finite temperatures. We confirmed the itinerant characteristics of Fe in Fe-Al-Si alloys. We also confirmed that the calculated exchange stiffness constant of the B2 structure is significantly small compared with that of other structures. However, calculated Curie temperatures are in the same order for all structure that are assumed in this work. In addition, we found that the Fe atoms that are closest to the Al and Si atoms exhibit smaller magnetic moments than other Fe atoms; this may reflect the itineracy of these Fe atoms owing to the strong hybridization with the $2p$ orbitals of Al and Si atoms. Moreover, the calculated temperature dependence of the exchange stiffness constant of the B2 structure is also unique; this might be related to the spin configuration dependence of the exchange interactions, which deviates from the behavior of the usual Heisenberg model. We also proposed that Si doping can increase the amplitude of the exchange stiffness constant.

ACKNOWLEDGMENTS

This work was supported by JSPS KAKENHI Grant Numbers JP19H05612 in Japan.

-
- [1] H. Masumoto and T. Yamamoto, *J. Jpn. Inst. Metals.* **1**, 127 (1937).
 - [2] S. Akamatsu, M. Oogane, M. Tsunoda, and Y. Ando, *AIP Adv.* **10**, 015302 (2020).
 - [3] S. Akamatsu, M. Oogane, M. Tsunoda, and Y. Ando, *Appl. Phys. Lett.* **120**, 242406 (2022).
 - [4] S. Akamatsu, B. H. Lee, Y. Hou, M. Tsunoda, M. Oogane, G. S. D. Beach, and J. S. Moodera, *APL* **12**, 021101 (2024).
 - [5] F. J. Dyson, *Phys. Rev.* **102**, 1217 (1956).
 - [6] U. Atxitia, D. Hinzke, O. Chubykalo-Fesenko, U. Nowak, H. Kachkachi, O. N. Mryasov, R. F. Evans, and R. W. Chantrell, *Phys. Rev. B* **82**, 134440 (2010).
 - [7] R. Moreno, R. F. L. Evans, S. Khmelevskiy, M. C. Muñoz, R. W. Chantrell, and O. Chubykalo-Fesenko, *Phys. Rev. B* **94**, 104433 (2016).
 - [8] L. M. Small and V. Heine, *J. Phys. F: Met. Phys.* **14** 3041 (1984).
 - [9] V. Heine, A. I. Lichtenstein, and O. N. Mryasov, *Europhys. Lett.* **12**, 545 (1990).
 - [10] M. U. Luchini and V. Heine, *Europhys. Lett.* **14**, 609 (1991).
 - [11] O. N. Mryasov, A. J. Freeman and A. I. Liechtenstein, *J. Appl. Phys.* **79**, 4805 (1996).
 - [12] T. Moriya, *Spin Fluctuations in Itinerant Electron Magnetism* (Springer, Berlin, 1985).
 - [13] M. Cyrot, *Phys. Rev. Lett.* **25**, 871 (1970).
 - [14] J. Hubbard, *Phys. Rev. B* **19**, 2626 (1979).
 - [15] J. Hubbard, *Phys. Rev. B* **20**, 4584 (1979).
 - [16] H. Hasegawa, *J. Phys. Soc. Jpn.* **46**, 1504 (1979).
 - [17] H. Hasegawa, *J. Phys. Soc. Jpn.* **49**, 178 (1980).
 - [18] H. Hasegawa, *J. Phys. Soc. Jpn.* **49**, 963 (1980).
 - [19] T. Oguchi, K. Terakura, and N. Hamada, *J. Phys. F* **13**, 145 (1983).
 - [20] A. J. Pindor, J. Staunton, G. M. Stocks, and H. Winter, *J. Phys. F* **13**, 979 (1983).
 - [21] J. Staunton, B. L. Gyorffy, A. J. Pindor, G. M. Stocks, and H. Winter, *J. Magn. Magn. Mater.* **45**, 15 (1984).
 - [22] B. L. Gyorffy, A. J. Pindor, J. Staunton, G. M. Stocks, and H. Winter, *J. Phys. F* **15**, 1337 (1985).
 - [23] J. B. Staunton and B. L. Gyorffy, *Phys. Rev. Lett.* **69**, 371 (1992).
 - [24] J. B. Staunton, S. Ostanin, S. S. A. Razee, B. L. Gyorffy, L. Szunyogh, B. Ginatempo, and E. Bruno, *Phys. Rev. Lett.* **93**, 257204 (2004).
 - [25] J. B. Staunton, L. Szunyogh, A. Buruzs, B. L. Gyorffy, S. Ostanin, and L. Udvardi, *Phys. Rev. B* **74**, 144411 (2006).
 - [26] A. Deák, E. Simon, L. Balogh, L. Szunyogh, M. dos Santos Dias, and J. B. Staunton, *Phys. Rev. B* **89**, 224401 (2014).
 - [27] M. Matsumoto, R. Banerjee, and J. B. Staunton, *Phys. Rev. B* **90**, 054421 (2014).
 - [28] S. Yamashita and A. Sakuma, *J. Phys. Soc. Jpn.* **91**, 093703 (2022).
 - [29] J. Bouaziz, C. E. Patrick, and J. B. Staunton, *Phys. Rev. B* **107**, L020401 (2023).
 - [30] S. Yamashita and A. Sakuma, *Phys. Rev. B.* **108**, 054411 (2023).
 - [31] C. D. Woodgate, C. E. Patrick, L. H. Lewis, and J. B. Staunton, *J. Appl. Phys.* **134**, 163905 (2023).
 - [32] R. Hiratsatsu, D. Miura, and A. Sakuma, *Appl. Phys. Express* **15**, 013003 (2021).

- [33] R. Hiramatsu, D. Miura, and A. Sakuma, *J. Phys. Soc. Jpn.* **92**, 044704 (2023).
- [34] A. Sakuma and D. Miura, *J. Phys. Soc. Jpn.* **91**, 084701 (2022).
- [35] A. Sakuma, To be published.
- [36] A. Sakuma, *J. Phys. Soc. Jpn.* **69**, 3072 (2000).
- [37] O. K. Andersen, Z. Pawłowska, and O. Jepsen, *Phys. Rev. B*, **34**, 5253 (1986).
- [38] I. Turek, V. Drchal, J. Kudrnovský, M. Šöb, and P. Weinberger, *Electronic Structure of Disordered Alloys, Surfaces and Interfaces* (Kluwer Academic, Dordrecht, 1997).
- [39] J. Kudrnovský and V. Drchal, *Phys. Rev. B*, **41**, 7515 (1990).
- [40] H. L. Skriver, *The LMTO Method* (Springer, Berlin, 1984).
- [41] A. I. Liechtenstein, M. I. Katsnelson, V. P. Antropov, and V. A. Gubanov, *J. Magn. Magn. Mater.* **67**, 65 (1987).
- [42] L. M. Sandratskii, *Phys. Status Solidi B* **136**, 167 (1986).
- [43] J. Kübler, *Theory of Itinerant Electron Magnetism* (Oxford University Press, New York, 2009).
- [44] O. N. Mryasov, V. A. Gubanov and A. I. Lichtenstein, *Phys. Rev. B*, **45**, 12330 (1992).
- [45] M. Uhl, L. Sandratskii, and J. Kübler, *J. Magn. Magn. Mater.* **103**, 314 (1992).
- [46] J. Kübler, *J. Phys.: Condens. Matter* **18**, 9795 (2006).
- [47] S. Yamashita and A. Sakuma, *Appl. Phys. Express* **16**, 083002 (2023).
- [48] S. Yamashita and A. Sakuma, *Jpn. J. Appl. Phys.* **63**, 025501 (2024).
- [49] M. Uhl and J. Kübler, *Phys. Rev. Lett.* **77**, 334 (1996).
- [50] N. M. Rosengaard and B. Johansson, *Phys. Rev. B* **55**, 14975 (1997).
- [51] S. V. Halilov, H. Eschrig, A. Y. Perlov, and P. M. Oppeneer, *Phys. Rev. B* **58**, 293 (1998).
- [52] A. V. Ruban, S. Khmelevski, P. Mohn, and B. Johansson, *Phys. Rev. B* **75**, 054402 (2007).
- [53] W. Wang, T. Ma, and M. Yan, *J. Alloys Compd.* **459**, 447 (2008).
- [54] T. Tanaka and Y. Gohda, *npj Comput. Mater.* **6**, 184 (2020).
- [55] M. Heine, O. Hellman, and D. Broido, *Phys. Rev. B* **100**, 104304 (2019).
- [56] G. Shirane, V. J. Minkiewicz, R. Nathans, *J. Appl. Phys.* **39**, 383 (1968).
- [57] T. Kubota, J. Hamrle, Y. Sakuraba, O. Gaier, M. Oogane, A. Sakuma, B. Hillebrands, K. Takahashi, and Y. Ando, *J. Appl. Phys.* **106**, 113907 (2009).
- [58] S. Khmelevskyi and P. Mohn, *J. Magn. Magn. Mater.* **560**, 169615 (2022).
- [59] S. Khmelevskyi, T. Khmelevska, A. V. Ruban and P. Mohn, *J. Phys.: Condens. Matter* **19**, 326218 (2007).

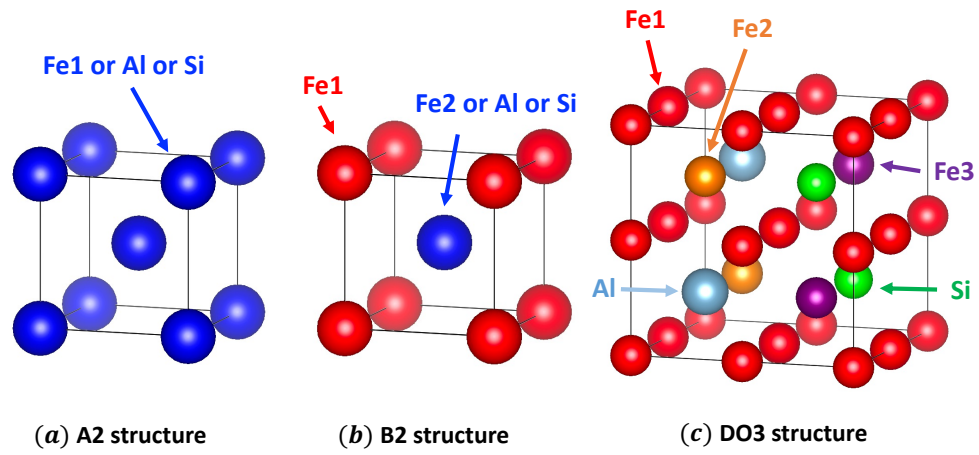


FIG. 1. Crystal structures of Fe-Al-Si alloy ($\text{Fe}_{75}\text{Al}_{12.5}\text{Si}_{12.5}$) assumed in this study.

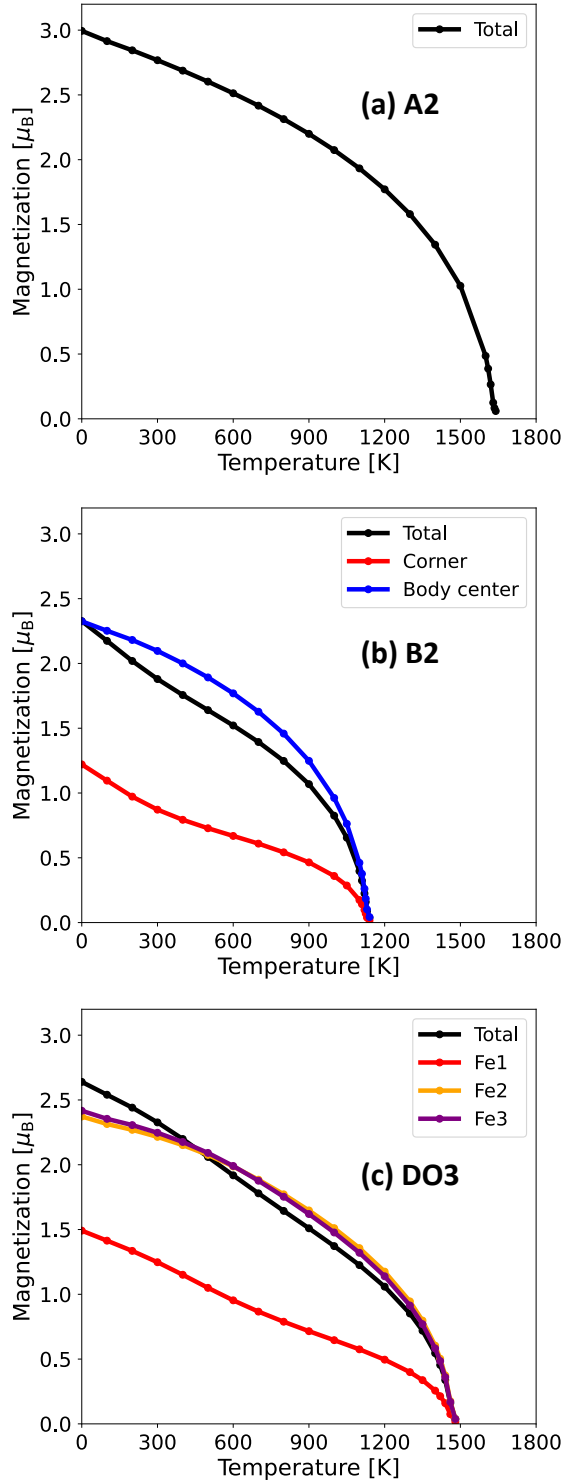


FIG. 2. Calculated temperature dependences of magnetization for (a) A2, (b) B2 and (c) DO3. The estimated Curie temperatures are 1160 K, 1640 K, and 1480 K for the A2, B2 and DO3 structures, respectively. For comparison, we scaled the total magnetization of the DO3 structure by 1/8. Temperature dependences of Fe sites resolved magnetization are also shown in (b) and (c).

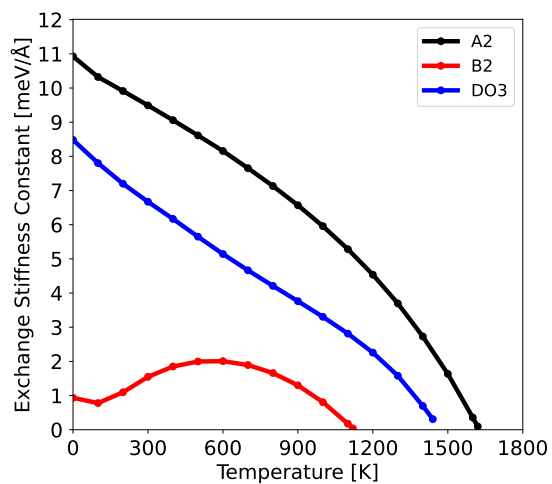


FIG. 3. Calculated temperature dependence of the exchange stiffness constants of Fe-Al-Si alloy with A2, B2, and DO3 structure.

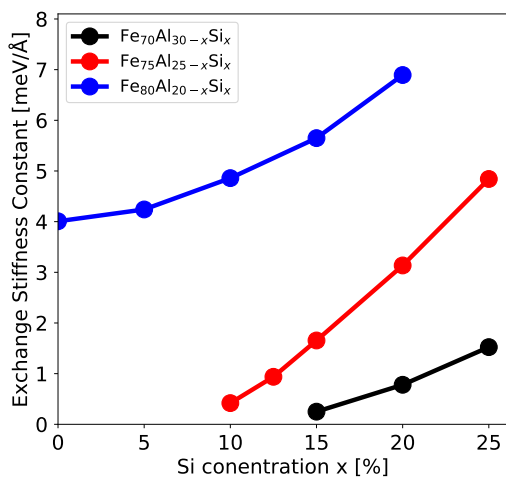


FIG. 4. Si concentration dependence of the exchange stiffness constant for the B2 structure at 0 K. The concentration of Fe increases from 70% to 80%.

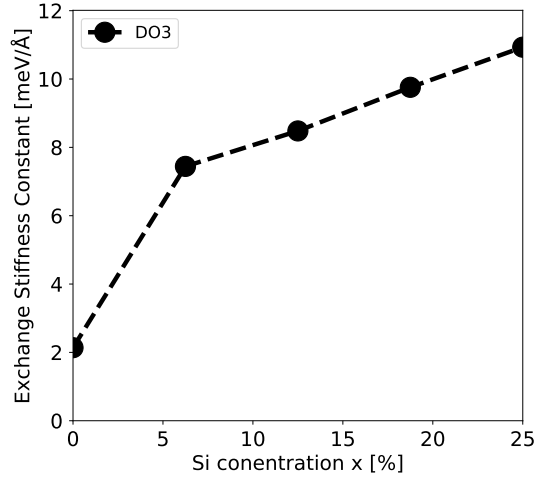


FIG. 5. Si concentration dependence of the exchange stiffness constant for the DO3 structure at 0 K.